



# Development of palladium-resin composites for catalytic hydrodechlorination of 4-chlorophenol

Nastaran Jadbabaie<sup>a</sup>, Tao Ye<sup>b</sup>, Danmeng Shuai<sup>b</sup>, Huichun Zhang<sup>a,\*</sup>

<sup>a</sup> Department of Civil and Environmental Engineering, Temple University, 1947 North 12th Street, Philadelphia, PA 19122, United States

<sup>b</sup> Department of Civil and Environmental Engineering, The George Washington University, 800 22nd St NW, Suite 3530, Science and Engineering Hall, Washington, DC 20052, United States

## ARTICLE INFO

### Article history:

Received 26 April 2016

Received in revised form

15 November 2016

Accepted 29 December 2016

Available online 30 December 2016

### Keywords:

Palladium nanoparticles

Polymeric resins

4-chlorophenol

Hydrodechlorination (HDC)

Adsorption

## ABSTRACT

Polymeric resins have been widely used for the removal of halogenated compounds, however, the sustainability of resin adsorption is compromised by frequent resin regeneration and further treatment/disposal of concentrated brine. Palladium (Pd)-based catalytic hydrogenation is promising to treat various classes of contaminants, including halogenated compounds, and the development of Pd-polymeric resin composites is advantageous because the composites can convert halogenated compounds to less toxic chemicals *in situ* and mitigate challenges associated with resin regeneration. In this work, three neutral resins (MN200, MN100, and XAD4) and two anion exchange resins (IRA910 and IRA96) were used as Pd supports to evaluate 4-chlorophenol (4-CP) hydrodechlorination reactivity. Similar 4-CP adsorption and reduction kinetics were observed, i.e., adsorption and reduction were both faster at acidic pHs for the neutral resins but faster at basic pHs for the anionic resins. The developed Langmuir–Hinshelwood kinetic model based on surface reaction as the rate determining step also suggested an enhancing effect of adsorption on the catalytic reactivity. When adsorption was constant, the reactivity of the catalysts increased with increasing solution pH. This is because higher pH mitigates the adverse impacts of the dehalogenation products (i.e., H<sup>+</sup> and Cl<sup>-</sup>) on the catalytic reaction. The inhibition effect of Cl<sup>-</sup> was more pronounced on IRA910 than on MN200. IRA910 with anion exchange functional groups facilitates Cl<sup>-</sup> adsorption and promotes the production of PdCl<sub>3</sub><sup>-</sup> and PdCl<sub>4</sub><sup>2-</sup> species, which are inactive for catalytic reduction. The accumulation of phenol, the dominant product in 4-CP reduction, on resin resulted in catalytic activity loss over eight cycles when 4-CP was repeatedly spiked into the same reactor; the catalytic activity was largely restored after resin regeneration.

© 2016 Elsevier B.V. All rights reserved.

## 1. Introduction

Chlorophenols (CPs) are among priority contaminants in water and wastewater effluents due to their high toxicity on human health (e.g., carcinogenic), adverse environmental impacts (e.g., inactivation of functional bacteria for the removal of organics), and persistence in the environment [1,2]. They are commonly found in the waste effluents of pesticide, dye, and wood preservative industries [1–4]. World-wide production of CPs is estimated at ca. 100,000 tons per year [5]. Moreover, CPs are biodegradation byproducts of complex molecules such as pesticides in the environment [6]. Conventional water treatment technologies such as ion exchange and adsorption by activated carbon or clays [7–9]

are used for the removal of CPs, however, these processes produce large amounts of concentrated brine or secondary waste through the regeneration of the absorbents [10–13]. Pd-based catalytic hydrogenation has recently emerged as a promising technology for reductive destruction of a broad spectrum of contaminants, including halogenated compounds (e.g., CPs, trichloroethylene, diatrizoate), oxyanions (e.g., nitrate, nitrite, bromate, chlorate, perchlorate), and N-nitrosamines [14–17]. Catalytic hydrogenation is beneficial for CP degradation because hydrogen is used as a clean reductant, CPs are converted to less toxic chemicals, secondary waste or byproduct generation is reduced, and catalysts can be reused over multiple cycles in principle [18].

Reduction of CPs has been mostly demonstrated by Pd nanoparticles loaded on supports including alumina and activated carbon [19–22]. However, fouling and stability loss over multiple catalytic cycles are major barriers in a widespread application of Pd-based catalysis [11,22]. For conventional catalyst supports such as acti-

\* Corresponding author.

E-mail address: [hjzhang@temple.edu](mailto:hjzhang@temple.edu) (H. Zhang).

vated carbon, both reactant and products (especially hydrophobic contaminants) may be strongly adsorbed to the support surface, which will inhibit the long-term performance of the catalyst. The non-selective adsorption of natural water constituents and foulants may compete with the contaminants for the reactive sites. In addition, catalyst selectivity for a target contaminant and production of desirable reaction products are additional important factors affecting the implementation of this technology [15]. Therefore, further efforts are required to develop alternative catalysts for cost-effective treatment of various classes of contaminants. Toward this end, the use of polymeric resins as catalyst supports is largely under-explored. On the other hand, polymeric resins have been extensively used to remove organic and ionic pollutants such as halogenated phenols from industrial wastewater effluents. Resins are advantageous because of their high surface area, enhanced porosity, and tunable pore size distribution and surface functional groups that can target the removal of specific contaminants [23–27]. These properties enable resins to be suitable support materials, especially when selectivity, long lifetime, ease of regeneration etc. are among important considerations. For example, resins with strong affinity to target contaminants may outperform conventional supports because catalytic reduction is a surface mediated reaction and the overall reactivity could be limited by contaminant adsorption on the catalyst [24,25,27]. This is especially beneficial for environmental applications in complex water matrices. Moreover, the immobilization of nanoparticles on resins can be enhanced by the presence of ionic functional groups and pores that promote electrostatic interactions and steric stabilization [28,29]. In addition, Pd enables the detoxification of CPs adsorbed on the resins and promotes *in situ* resin regeneration.

Several pioneer studies demonstrated the advantages of using resin supported Pd for catalytic hydrogenation of anions, but none examined the removal of halogenated compounds. In a study by Kim and Choi, a Pd-supported ion-exchange resin was developed for complete decomposition of perchlorate through adsorption onto a strong anion exchange resin followed by catalytic decomposition of the adsorbed  $\text{ClO}_4^-$  [30]. Nitrate reduction by bimetallic catalysts on cation and anion exchange resins was also investigated [12,31–34]. The results showed that the activity of the catalysts on the anion exchange resin was higher than that on the cation exchange resin. This is mainly due to the electrostatic attraction between  $\text{NO}_3^-$  and the functional groups of the anion exchange resin. In these studies, however, the adsorbed amounts of the target contaminants by the resins during the catalytic reactions were not tested. Therefore, it is difficult to attribute the decrease in soluble contaminant concentrations to either catalytic reduction or adsorption. In a few other studies, a combination of adsorption and catalytic reduction has been investigated to treat secondary waste streams of used resins [35,36]. Ion exchange onto anion exchange resins and catalytic reduction by bimetallic catalysts ( $\text{Pd-Cu/Al}_2\text{O}_3$  and  $\text{Re-Pd/C}$ ) have been coupled to remove nitrate and perchlorate from contaminated water and to treat and reuse the regenerant brine [35–37]. The main advantage of this method is elimination of the secondary waste stream, but it still requires operation of ion exchange, resin regeneration, and catalytic reduction in different reactors.

Therefore, it is important to explore the possibility of simultaneous removal of contaminants and regeneration of Pd-loaded resins. One solution is to design Pd loaded resin catalysts with different adsorption affinity for the parent contaminant and the reduction product(s), i.e., to convert a target contaminant with high adsorption affinity to reduction product(s) with low adsorption affinity. The high adsorption affinity of the target contaminant enhances contaminant removal (i.e., adsorption and then catalytic reduction), and the reduction products with low adsorption affinity to the cata-

lyst support can be easily released to the aqueous phase to minimize the need for resin regeneration.

The main goal of this work was to develop novel Pd-based catalysts supported on polymeric resins, and to provide mechanistic insight into the catalytic reduction of CPs and the possibility of *in situ* regeneration of the resins. Two groups of resins including anion exchange resins and neutral resins with different structures and functional groups were selected to identify the key physical and chemical properties of the resins for impacting the catalytic activity, catalyst longevity, and the poisoning effect of  $\text{Cl}^-$ . The catalysts were characterized by transmission electron microscopy (TEM) to determine Pd nanoparticle size distribution, energy dispersive X-ray spectroscopy (EDX) to analyze the surface composition of the catalysts, and X-ray powder diffraction (XRD) to evaluate the crystallinity of the nanoparticles. Ion exchange capacity and Brunauer-Emmett-Teller (BET) surface area of the resins were measured before and after Pd loading. 4-Chlorophenol (4-CP) was selected as the target contaminant for removal. Effects of pH and  $\text{Cl}^-$  and 4-CP concentrations on the reactivity of the catalysts were examined to investigate the poisoning effect of  $\text{Cl}^-$  and to develop kinetic modeling. Longevity and the possibility of *in situ* regeneration of the catalysts over multiple cycles of 4-CP removal was also investigated, under extreme conditions where a high concentration of 4-CP (1 mmol L<sup>-1</sup>) was repeatedly spiked into the same reactor.

## 2. Materials and methods

### 2.1. Materials and chemicals

Three nonionic polymeric resins, cross-linked Amberlite XAD-4 and hyper-cross-linked MN200 and MN100, were provided by Rohm and Hass (U.S.) and Purolite® (U.S.), respectively. MN200 and XAD-4 have similar polystyrene structures, but MN200 has a higher degree of cross-linkage which results in a larger surface area and additional micropores. The difference between MN200 and MN100 is that MN200 does not have any functional groups while MN100 has a small fraction of tertiary amine functional groups, with an ion exchange capacity of 0.1–0.3 meq/g (reported by the manufacturer). Two polystyrene-based anion exchange resins (AXRs), Amberlite IRA910 and IRA96, were obtained from Dow® (U.S.). IRA910 is strongly basic with dimethyl-ethanolammonium functional groups. IRA96 is weakly basic with tertiary amine functional groups. Analytical grade 4-CP,  $\text{NaPdCl}_4$ , and  $\text{NaBH}_4$  were purchased from Fisher Scientific and Sigma-Aldrich and used without further purification. The 4-CP solution was prepared with ultrapure deionized water. Ultra high purity hydrogen gas ( $\text{H}_2$ –99.999%) was supplied by Air Gas.

### 2.2. Catalyst preparation

Resin beads were soaked in a  $\text{NaPdCl}_4$  solution, mixed gently overnight (300 rpm for at least 12 h), and collected after filtration.  $\text{NaPdCl}_4$  was adsorbed onto the resin surface, and a nominal loading of 1% Pd (by weight) was achieved. Next, the  $\text{NaPdCl}_4$  adsorbed resins were re-suspended in ultrapure water, and a  $\text{NaBH}_4$  solution (pH 12) was added dropwise under violent stirring (600 rpm). The molar ratio of  $\text{NaBH}_4$  to  $\text{NaPdCl}_4$  was 20, in excess to the stoichiometric ratio to convert all Pd precursors into  $\text{Pd}^0$ . The reaction lasted for 2 h, and the resins were collected by filtration and rinsed thoroughly with ultrapure water to remove free Pd particles from the resins. The actual Pd loading was determined by inductively coupled plasma-optical emission spectroscopy (ICP-OES). In order to find the optimum cleaning procedure for the catalysts, the 1% Pd/resins were washed with ultrapure water for three additional times, and some resin beads were harvested for catalytic activity

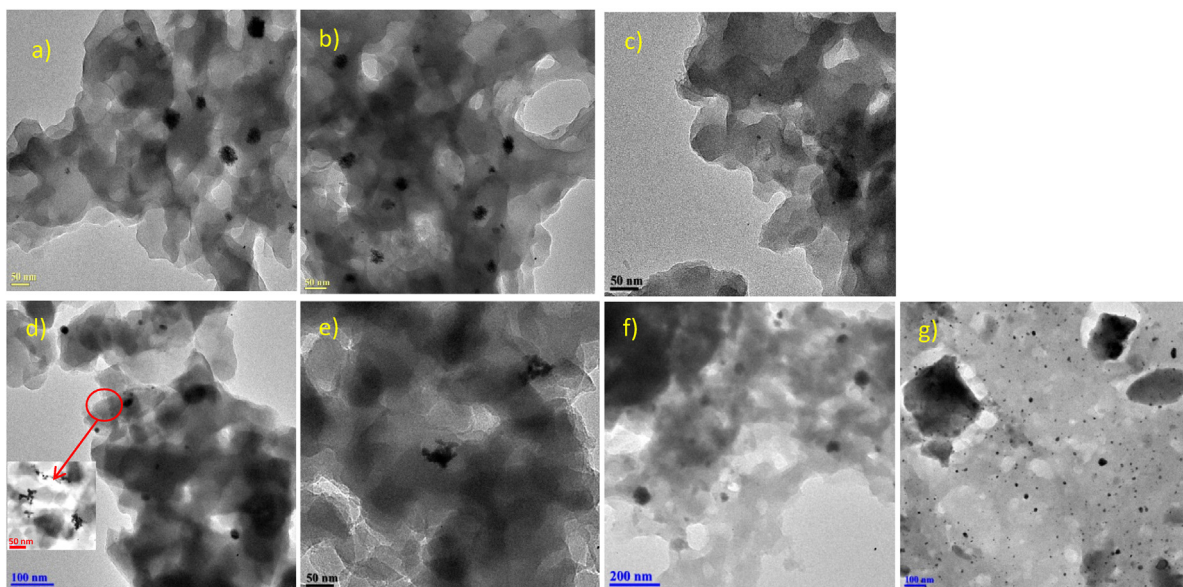


**Fig. 1.** TEM images of a) fresh 1% Pd/IRA910, b) used 1% Pd/IRA910, c) Pd/IRA96, d) fresh 1% Pd/MN200, e) used 1% Pd/MN200, f) 1% Pd/MN100, and g) 1% Pd/XAD4.

tests after each wash. The results of the reduction experiments at pH 3 and 11 indicated that the reactivity of Pd/MN200 and Pd/IRA910 catalysts decreased after two-time washing in comparison with one-time washing. This is due to the removal of some free or loosely attached  $Pd^0$  particles after washing. Further washing did not affect reactivity, therefore, resins washed twice were used for all reduction experiments.

### 2.3. Experimental setup

The semi-batch reduction experiments were carried out in 100 mL three-neck round bottom flasks at ambient temperature ( $22 \pm 1^\circ C$ ), with a continuous flow of hydrogen gas ( $50 \text{ mL min}^{-1}$ ) and a mixing rate of 500 rpm (Fig. S1 in the Supplementary Material (SM)). The hydrogen supply and mixing have been optimized to deliver sufficient reductant and minimize mass transfer limitations. One flask port was used to supply hydrogen, one for collecting samples, and one for venting the off-gas. Silicon rubber stoppers were used to seal the reactors to prevent hydrogen leakage into the atmosphere. First, 60 mL distilled water was added to the flask, then pH of the solution was adjusted to the desired value.  $1 \text{ mol L}^{-1}$  of HCl solution,  $1 \text{ mol L}^{-1}$  of acetic acid buffer,  $0.1 \text{ mol L}^{-1}$  of phosphate buffer, or  $1 \text{ mol L}^{-1}$  of NaOH solution was used to adjust solution pH to 3, 5, 7, and 11, respectively. Next, an appropriate amount of the catalysts was added to the solution (i.e., to achieve a Pd loading of  $2.5 \text{ mg L}^{-1}$ ), and the catalyst was pre-sparged with hydrogen gas for 30 min to restore the catalyst activity. Pd-based catalysts may be oxidized in air under ambient conditions, sparging hydrogen gas was shown to sufficiently restore the catalytic activity [14]. 4-CP solution was then amended to initiate reduction. Supernatants (0.5 mL) were collected at regular time intervals during the 150-min reaction.

Desorption experiments were carried out to determine the amount of 4-CP adsorbed by the catalysts during reaction. For the desorption experiments, the catalysts collected at different reaction times were filtered and transferred to amber glass bottles with Teflon-lined screw caps. Methanol (20 mL) was added for neutral resins, and a mixture containing methanol, water, and NaCl (20 mL, methanol/water = 1/1 by volume, 8% NaCl by weight) was used for ionic resins. The amber bottles were shaken under 175 rpm for 48 h, and 0.5 mL supernatants were taken for the analysis of contami-

nant and product concentrations. The catalysts were also reused to study their longevity. In these cyclic experiments,  $1 \text{ mmol L}^{-1}$  of 4-CP was repeatedly spiked to the reaction solution every three hours for eight reduction cycles (preliminary experiments showed that 4-CP was completely removed within three hours). Batch experiments for 4-CP adsorption onto the catalysts were carried out in a similar way except that hydrogen gas was not present.

### 2.4. Analytical method

4-CP and phenol were analyzed using Agilent Technologies 1200 Infinity Series high-performance liquid chromatography (HPLC) with a Zorbax XDB-C18 column. A mobile phase composed of 70% methanol and 30% diluted phosphoric acid at pH 3.0 and a flow rate of  $1 \text{ mL min}^{-1}$  was used. The diode array detector was set to 273 nm for phenol and 282 nm for 4-CP to determine their concentrations.

### 2.5. Characterization

TEM analysis was carried out with a JEOL JEM-1400 coupled with an energy dispersive X-ray spectrometer to determine Pd nanoparticle size distribution and to perform elemental analysis. To prepare samples, the resin beads were crushed finely and dispersed in methanol, and then deposited on a carbon/Cu grid. The samples were then dried under room temperature. XRD was used to characterize the crystallinity of the catalysts. A Bruker Kappa APEX II DUO single crystal X-ray diffractometer was used for collecting XRD data. The BET surface area of the resins was measured using a nitrogen gas adsorption apparatus. The Pd loading of the catalysts was measured using ICP-OES after digestion in concentrated nitric acid and hydrochloric acid (3050B EPA method).

### 2.6. Mass transfer limitation

Both extra- and intra-particle mass transfer rates were evaluated to determine whether the measured catalytic activity is limited by mass transfer. The extra-particle liquid-solid mass transfer rate was evaluated by calculating the overall liquid-solid mass transfer rate coefficient,  $k_c$ , based on the slip velocity approach of

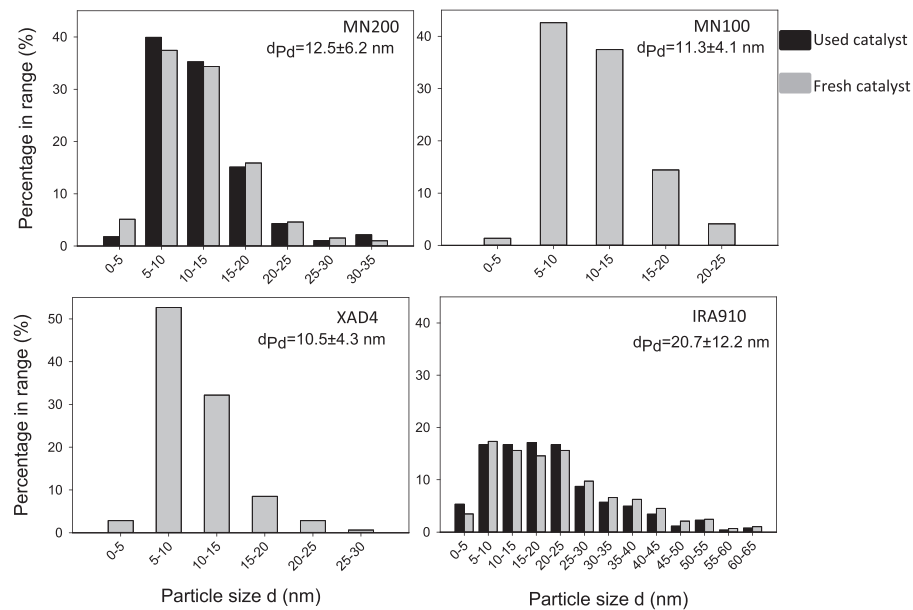


**Fig. 2.** Particle size distribution of the fresh 1% Pd/catalysts and used 1% Pd/catalysts after eight times of usage.

Hariott [38]. The transfer rate for single spheres is given by the semitheoretical equation:

$$N_{Sh} = \frac{k_c D_p}{D_v} = 2 + 0.6 \left( \frac{D_p v \rho}{\mu} \right)^{0.5} \left( \frac{\mu}{\rho D_v} \right)^{0.33} \quad (1)$$

where  $N_{Sh}$  is the Sherwood number,  $D_p$  is the particle diameter,  $D_v$  is the diffusivity coefficient of the compound in water as estimated by the Hayduk and Laudie method,  $v$  is the fluid mean velocity,  $\rho$  is the liquid density, and  $\mu$  is the liquid dynamic viscosity. The mass transfer rate constant was then calculated by multiplying the mass transfer coefficient ( $k_c$ ) by the geometric surface area of the catalyst per volume of the solution,  $a$ :

$$a = \frac{\text{total surface area}}{\text{total volume}} = \frac{SA_p \times M}{\rho_p \times V_p} \times \frac{1}{V_R} \quad (2)$$

where  $SA_p$  and  $V_p$  are the geometric surface area and volume of one particle,  $M$  is the mass of the catalyst in the reactor,  $\rho_p$  is the catalyst particle density, and  $V_R$  is the reactor volume. In order to evaluate intraparticle liquid-solid mass transfer limitation, the Weisz and Prater criterion [39], which is the ratio of the reaction rate to the diffusion rate, was used:

$$\frac{k_{obs} D_p^2}{D_e} \quad (3)$$

where  $k_{obs}$  is the observed reaction rate constant and  $D_e$  is the effective diffusivity which was approximately calculated as  $0.02 D_v$  [40]. When the Weisz and Prater criterion is less than 1, the intraparticle mass transfer resistance is negligible.

### 3. Data analysis

#### 3.1. Reaction kinetics

The removal of 4-CP by all the catalysts follows pseudo-first-order kinetics:

$$\frac{dC}{dt} = -k_{obs} C \quad (4)$$

where  $C$  is 4-CP concentration ( $\mu\text{mol L}^{-1}$ ) in solution phase and  $k_{obs}$  ( $\text{min}^{-1}$ ) is the observed pseudo-first order reaction rate constant.

The rate constants were obtained from the linear regression of the natural log of solution phase concentration versus time.

#### 3.2. Turnover frequency (TOF<sub>0</sub>)

The initial turnover frequency values (TOF<sub>0</sub>,  $\text{min}^{-1}$ ), the number of molecules reduced per site per minute, were determined by dividing the product of the observed rate constant ( $k_{obs}$ ,  $\text{min}^{-1}$ ) and the initial 4-CP concentration ( $C_0$ ,  $\text{mol L}^{-1}$ ) by the concentration of surface Pd ( $C_{\text{surface-Pd}}$ ,  $\text{mol L}^{-1}$ ), as following [41]:

$$TOF_0 = \frac{k_{obs} C_0}{C_{\text{surface-Pd}}} = \frac{k_{obs} C_0 M}{C_{Pd} D} \quad (5)$$

where  $C_{\text{surface-Pd}}$  is the product of Pd loading ( $C_{Pd}$ ,  $\text{g L}^{-1}$ ) and dispersion divided by the Pd atomic weight ( $M$ ,  $106.4 \text{ g mol}^{-1}$ ). Preliminary TEM analyses suggested that Pd nanoparticles were near-spherical, and hence the nanoparticle shape was approximated by cuboctahedron [15]. The dispersion of cuboctahedrons is calculated by [15]:

$$D = \frac{30v^2 + 6}{10v^3 + 15v^2 + 11v + 3} \quad (6)$$

where  $v$  is the average order of cuboctahedral nanoparticles and calculated by:

$$v = \frac{d}{2d_{\text{metal-metal}}} - \frac{1}{2} \quad (7)$$

where  $d$  is the nanoparticle diameter obtained from TEM analysis, and  $d_{\text{metal-metal}}$  is the distance between metal atoms which is equal to  $0.275 \text{ nm}$  for Pd.

## 4. RESULTS and DISCUSSION

#### 4.1. Characterization of the catalysts

The actual Pd content, BET surface area, and ion exchange capacity of the resins before and after loading 1 wt% Pd are listed in Table 1. The BET surface areas of the neutral resins and the ion exchange capacities of IRA96 and MN100 did not change significantly after loading Pd. The ion exchange capacity of IRA910 decreased by 17% after loading 1 wt% Pd. TEM images and particle

**Table 1**

Properties of the catalysts.

Resin Pd nominal weight	% Pd	Exchange capacity (meq/g)		BET surface area ( $\text{m}^2/\text{g}$ )	
		Before <sup>a</sup>	After <sup>b</sup>	Before <sup>a</sup>	After <sup>b</sup>
MN200 1%	0.67	–	–	937	920
MN200 0.2%	0.14	–	–	–	–
MN200 0.5%	0.44	–	–	–	–
MN100 1%	0.78	0.4	0.5	811	783
XAD4 1%	0.11	–	–	829	832
IRA910 1%	0.76	5.3	4.4	–	21
IRA96 1%	0.31	6.2	6.1	–	–

<sup>a</sup> Before loading 1 wt% Pd.<sup>b</sup> After loading 1 wt% Pd.

size distributions are presented in Figs. 1 and 2. To obtain particle size distribution, the diameters of at least 200 individual Pd particles at different locations were measured for each catalyst. The surface-area-weighted average size  $d_{\text{Pd}}$  was calculated according to [30,42]:

$$d_{\text{Pd}} = \frac{\sum_i n_i d_i^3}{\sum_i n_i d_i^2} \quad (8)$$

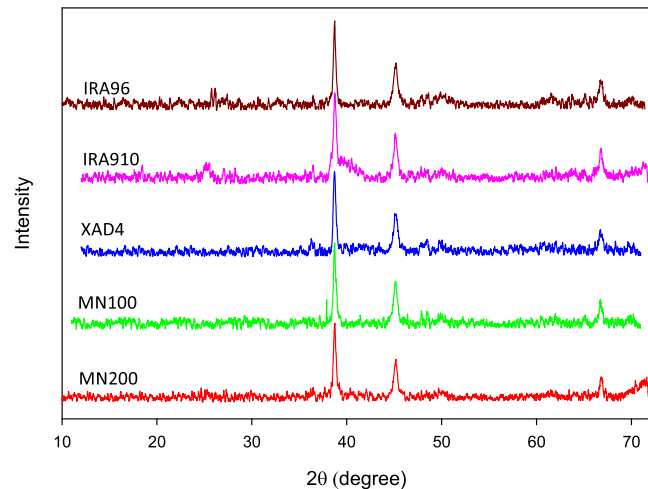
where  $n_i$  is the number of particles of diameter  $d_i$ .

TEM and EDS results of the catalysts illustrated that Pd nanoparticles were highly dispersed in the porous structure of the resins. MN200, IRA910, and MN100 showed similar dispersion of Pd nanoparticles, mostly nanoclusters with some nanoparticles present. The nanoclusters are distributed non-uniformly within the resin structures. TEM images of XAD4 exhibited dispersion of mostly Pd nanoparticles with more uniform distribution and less nanoclusters, however, its particle size distribution was similar to the other two neutral resins. Note the much lower actual Pd loading on XAD4 compared to the other resins, even though with the same theoretical loading of 1 wt% (Table 1). TEM images of IRA96 showed very poor dispersion of Pd nanoparticles. The low reactivity of this catalyst can be related to the low  $\text{Pd}^0$  loading of 0.31 wt% (the highest rate constant was measured to be  $0.003 \text{ min}^{-1}$  at pH 11 for IRA96). The macroporous structure of XAD4, whose proportion of macropores (pore size between 2 nm to 50 nm) is 86.8% of the total pore volume, has resulted in higher dispersion of Pd nanoparticles on the resin structure than on MN200. MN200 has a microporous structure, whose proportion of micropores (pore size < 2 nm) is 69.5% of the total pore volume. This difference is due to the easier access of Pd precursors to larger pores. Pd particles supported on IRA910 exhibited a broader size range and larger particle sizes comparing to the neutral resins, but the detailed mechanism requires further exploration. Pd particle dispersion in MN200 and IRA910 did not change after repeated usage (Fig. 2).

The X-ray diffraction (XRD) patterns of the catalysts were in agreement with the  $\text{Pd}^0$  crystal reference pattern and  $\text{Pd}^0$  was the only observed crystalline phase (Fig. 3).

#### 4.2. Mass transfer

Extra- and intra-particle mass transfer rates of a reactant can influence its catalytic activity [43]. Particle size and mixing rate in reaction are two major factors that can control mass transfer rates. Higher mixing rates and smaller particle sizes lower the likelihood of mass transfer limitation [44]. The calculated external mass transfer rate constants were smaller than the measured  $k_{\text{obs}}$  for all the catalysts (Table 2). This indicates that liquid-solid mass transfer rate could limit the measured reactivity. An explanation for the observed extra-particle mass transfer limitation is that the resin beads are large particles ( $D_p > 500 \mu\text{m}$ ). In addition, the calculation is conservative because it underestimates the contribution

**Fig. 3.** XRD patterns of the palladium nanoparticles deposited on the resins.**Table 2**

Extra-particle liquid-solid mass transfer rate constants ( $a \times k_c$ ), experimentally measured reaction rate constants ( $k_{\text{obs}}$ ), and Weisz and Prater criterion ( $k_{\text{obs}} D_p^2 / D_e$ ) for evaluating intra-particle liquid-solid mass transfer at pH 7 and 11 for neutral resins and AXRs, respectively. These pH values were selected because, as shown later, the resins had the highest reactivity under these pH conditions.

Resin	$a \times k_c (\text{s}^{-1})$	$k_{\text{obs},\text{max}} (\text{s}^{-1})$	$\frac{k_{\text{obs}} D_p^2}{D_e}$
MN200	$5.0 \times 10^{-5}$	$2.4 \times 10^{-4}$	$1.2 \times 10^{-1}$
XAD4	$3.0 \times 10^{-5}$	$1.5 \times 10^{-4}$	$9.4 \times 10^{-2}$
MN100	$7.0 \times 10^{-5}$	$1.8 \times 10^{-4}$	$1.3 \times 10^{-1}$
IRA910	$7.0 \times 10^{-5}$	$1.1 \times 10^{-3}$	$1.8 \times 10^{-1}$
IRA96	$5.0 \times 10^{-5}$	$8 \times 10^{-5}$	$6.1 \times 10^{-2}$

of mixing to the mass transfer rate (i.e., calculated based on the slip velocity of particles, only considering gravitational sedimentation) and of porous structure to mass transfer (i.e., considering resins as solid spheres without pores). Larger reaction rate constants were observed when the catalyst beads were crushed (data not shown), confirming the existence of external mass transfer limitation. Though crushing resin beads improved the catalytic activity for contaminant removal, we did all other experiments with uncrushed resins to best simulate the application of resins in water treatment practices. For the commercially available resins with particle sizes larger than  $500 \mu\text{m}$ , the external mass transfer limitation is inevitable and should be considered for catalyst development and evaluation.

The estimated values of the Weisz and Prater criterion were less than 1 for all catalysts (Table 2). This suggests that the rate of 4-CP reduction on the Pd surface is much slower than its diffusion through the internal pores. Thus, the intraparticle mass transfer limitation is negligible.

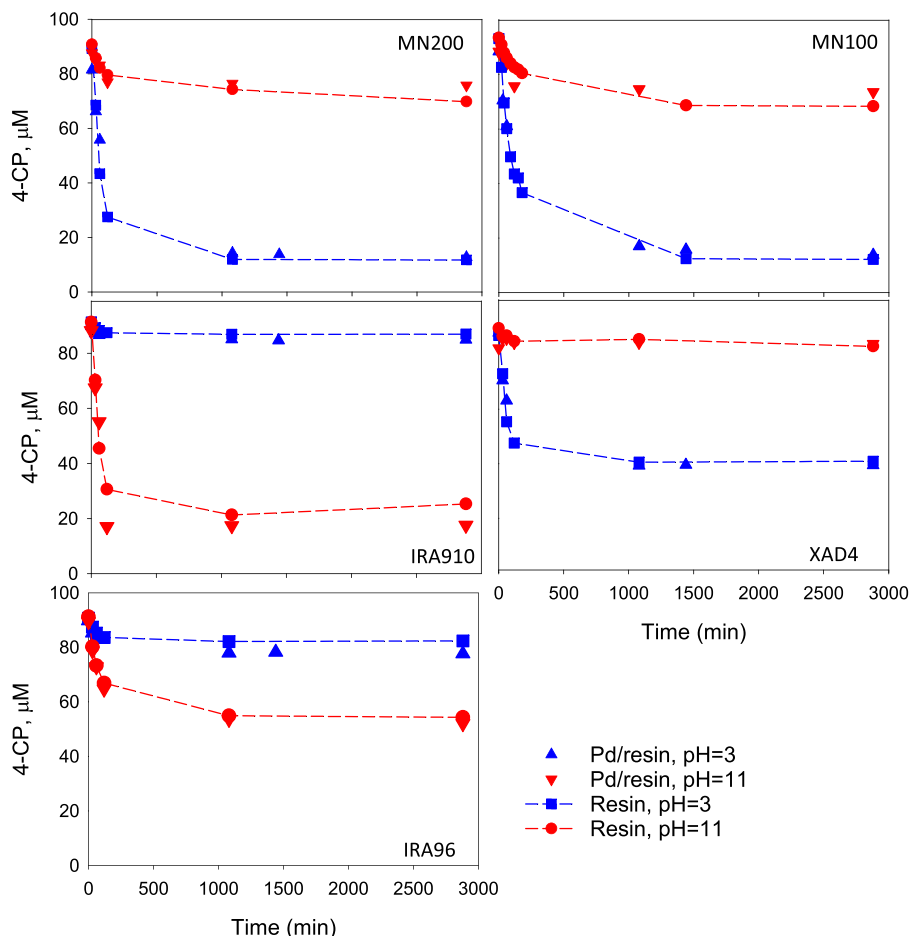


**Fig. 4.** Comparing adsorption capacity of the resins before and after loading 1 wt% Pd. Reaction conditions: initial 4-CP concentration of 100  $\mu\text{M}$ , 25 mg of resin or 25 mg of 1 wt% Pd catalyst loading, no  $\text{H}_2$  gas.

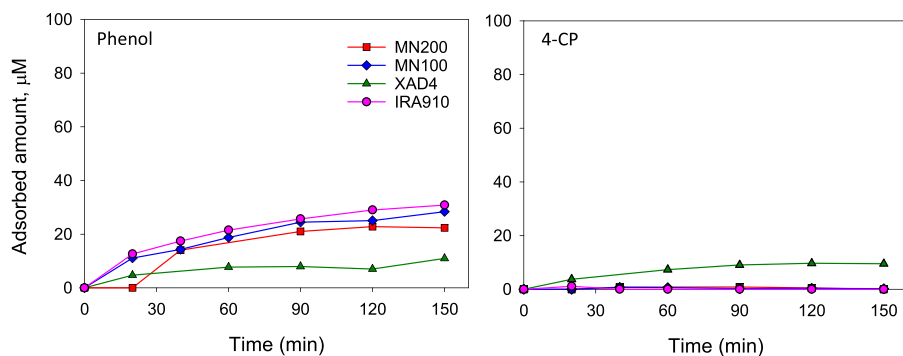


**Fig. 5.** Adsorbed amounts of phenol and 4-CP onto MN200, MN100, and XAD4 at pH 7 and onto IRA910 at pH 11 during the reaction. Reaction conditions: initial 4-CP concentration of 100  $\mu\text{M}$  and 25 mg of 1 wt% Pd catalyst loading.

#### 4.3. Adsorption properties

The adsorption results of 4-CP on the resins indicated that the adsorption capacity of the resins did not change much after loading 1 wt% Pd (Fig. 4). Similar to the original resins, 4-CP was significantly adsorbed by the catalysts supported on the neutral resins (MN200, MN100, and XAD4) at  $\text{pH} < \text{pK}_a$  (p $K_a$  of 4-CP is 9.1), where the non-dissociated form (i.e., protonated form) of 4-CP is the dominant species and has a higher adsorption affinity than the dissociated form (i.e., anionic form). The opposite is true for the adsorption of 4-chlorophenolate to the anion exchange resins (i.e., IRA910

and IRA96) at  $\text{pH} > \text{pK}_a$  when 4-chlorophenolate is the dominant species. These results verify the fact that neutral resins exhibit much higher adsorption capacities toward neutral compounds, while anion exchange resins have higher adsorption capacities toward anionic compounds. Generally, MN200 and MN100 showed greater adsorption capacity than XAD4. The larger amount of micro-pores in MN200 and MN100 enhance adsorption energies due to the superposition of the force fields of the opposite walls [45]. As will be shown later, the different adsorption capacities of the resin supports have large effects on the overall catalytic reduction of 4-CP.

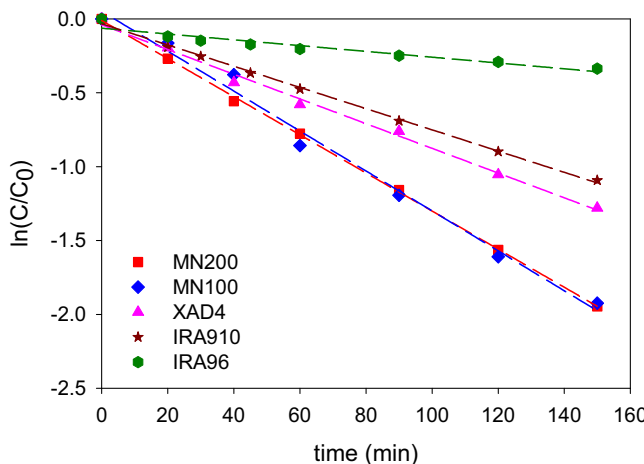


**Fig. 6.** Linear correlation between the natural log of 4-CP concentration in solution phase versus time for the experiment of 25 mg of 1 wt% Pd/resin at pH 7. The initial concentration of 4-CP was 0.1 mM.

#### 4.4. Reduction kinetics

The activity of the developed catalysts in the reduction of 4-CP was measured at different pHs. The hydrodechlorination of 4-CP over the catalysts mainly resulted in the formation of phenol. After catalytic reaction, the sum of soluble and adsorbed 4-CP and phenol accounts for more than 95% of the initial amount of 4-CP. For example, SM Fig. S2 shows the time course of 4-CP reduction, phenol formation, and the sum of 4-CP and phenol for XAD4 and IRA910. The amount of 4-CP and phenol adsorbed during reduction was measured by conducting reduction experiments in multiple reactors. The catalysts in each reactor were sacrificed for the desorption experiment at different reaction times. The desorption results in Fig. 5 confirmed that the 4-CP removal from solution by 1 wt% Pd-MN200, –MN100, and –IRA910 was resulted from reduction rather than from adsorption onto the resins (less than 1%). Up to 9% of 4-CP was adsorbed by 1 wt% Pd-XAD4 during the reaction. Phenol, however, was adsorbed onto all the resins during the reaction (Fig. 5). At pH 7, the amount of phenol adsorbed was the highest onto the MN200 and MN100 catalysts (30–40% of the total formed phenol), and for XAD4 was 11%. Phenol was moderately adsorbed onto IRA910 (about 34% of the total formed phenol) at pH = 11 when phenolate is the dominant species ( $pK_a$  of phenol is 10.0). Due to the negligible amount of 4-CP adsorbed during most of the reactions, pseudo-first-order rate constants for 4-CP reduction were obtained from the linear regression of the natural log of solution phase concentrations versus time (Fig. 6).

#### 4.5. Effect of pH on catalytic activity

4-CP reduction rate constants ( $k_{obs}$ ) for all catalysts at different pHs are shown in Fig. 7a, where  $k_{obs}$  typically increased with pH increasing from 3 to 7. Different behavior was observed for 4-CP reduction at pH 11, that is,  $k_{obs}$  for the catalysts supported on the neutral resins decreased when pH reached 11 while a significant increase was observed for the catalyst supported on IRA910. The initial turnover frequencies ( $TOF_0$ ) also followed the same trend (Fig. 7b). Solution pH affects both Pd activity and adsorption properties of the resins. Comparing the reduction and adsorption results suggested that faster reactivity is consistent with higher adsorption capacity for all the catalysts, as detailed below.

As illustrated in Fig. 8, the faster reduction of 4-CP on MN200 at pH 3, 5, and 7 than at pH 11 is compatible with its higher adsorption capacity/kinetics at the lower pH values. A similar enhancing effect

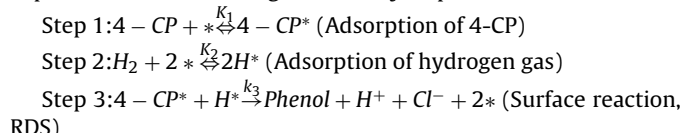
of adsorption on reduction was also observed for the reduction of 4-CP by IRA910 at pH 11 as compared to pH 3, 5, and 7. Thus, the ability of the catalysts to adsorb 4-CP molecules, which further react with activated hydrogen, facilitated the subsequent reduction of 4-CP.

In addition to affecting adsorption, solution pH also influences catalyst activity [46]. The activity of the catalysts increased with an increase in solution pH from 3 to 7 when the adsorption capacity of the resins was constant for both 4-CP and phenol. This is because 4-CP and phenol, with respective  $pK_a$  of 9.1 and 10.0, are both non-dissociated at these pHs. As reported by other studies, increasing pH enhances the conversion rate of 4-CP due to the mitigation of  $H^+$  and  $Cl^-$  inhibition [11,19], which are the byproducts of 4-CP reduction. High concentrations of  $Cl^-$  at low pH are favorable for  $PdCl_3^-$  and  $PdCl_4^{2-}$  formation. These anionic Pd species are inactive for 4-CP reduction, in contrast to  $Pd^{n+}$  species that were found to be important for dehalogenation [11,19,20]. The formation of  $PdCl_3^-$  and  $PdCl_4^{2-}$  also results in the leaching of Pd into aqueous solution, which further decreases the catalytic activity and compromises the longevity of the catalysts over multiple cycles.

#### 4.6. Kinetic modeling and effect of initial 4-CP concentration

In the reported mechanisms, hydrodechlorination of chlorinated organic compounds can be described by the following three steps: 1) adsorption of the target compound and hydrogen gas ( $H_2$ ) onto the catalyst surface ( $Pd^0$ ), typically following the Langmuir adsorption isotherm, 2) dissociation of the adsorbed hydrogen by metallic Pd and conversion to the adsorbed atomic hydrogen ( $Pd-H_{ads}$ ), and 3) reaction between the adsorbed atomic hydrogen and the co-adsorbed compound [47,48]. A kinetic model was developed for the reaction kinetics assuming surface reaction is the rate-determining step (RDS) based on the Langmuir-Hinshelwood (L-H) model which has been extensively applied to investigating heterogeneous catalytic processes [49–51]. Note that although reaction may be limited by the external mass transfer, the calculated mass transfer rates are not significantly smaller than the measured reactivity (Table 2). The pre-determined RDS of 4-CP reaction or adsorption will simplify the developed L-H model and provides a reasonable estimate of the effects of 4-CP initial concentration on the catalytic activity. A more comprehensive L-H model analysis will be explored in the future for understanding the mechanism and 4-CP reduction, and experimental or simulation tools will be used to determine equilibrium constants and reaction rate constants that are essential for modeling.

When surface reaction is the RDS, the L-H model can be expressed as the following elementary steps:



where the active sites for chemisorption on the catalyst surface are described by \*. 4-CP\* and H\* are the chemisorbed 4-CP and hydrogen on the active surface sites, and phenol, H<sup>+</sup>, and Cl<sup>-</sup> are the reaction products. K<sub>1</sub> and K<sub>2</sub> are the equilibrium adsorption constants for 4-CP and H<sub>2</sub> respectively, and k<sub>3</sub> is the overall reaction rate constant.

Assuming negligible adsorption of phenol, H<sup>+</sup>, and Cl<sup>-</sup> due to low concentrations of the products at the beginning of the reaction, and noncompetitive equilibrium adsorption of 4-CP and H<sub>2</sub>, the L-H kinetic model can be expressed as [50,52]:

$$r_0 = k_r \left( \frac{K_1[4 - CP]_0}{(K_1[4 - CP]_0 + 1)} \right) \quad (9)$$

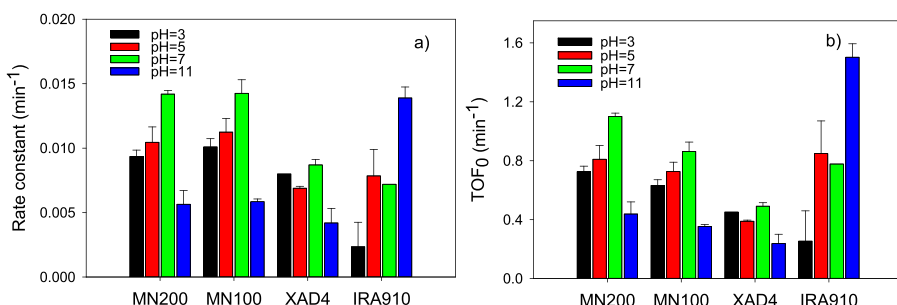


**Fig. 7.** Catalytic 4-CP reduction rate constants (a) and initial turnover frequency ( $\text{TOF}_0$ ) (b) over the catalysts at different pHs, initial 4-CP concentration of 100  $\mu\text{M}$ , and 25 mg of 1 wt% Pd catalyst loading.

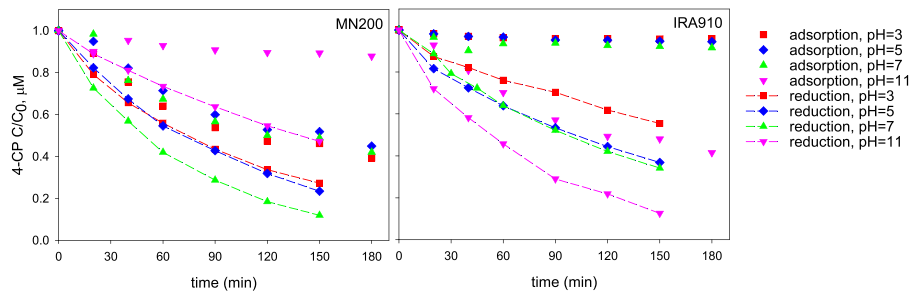


**Fig. 8.** Comparing the reduction and adsorption kinetics at different pHs (pH 3 and, 5, 7, and 11) for 25 mg of 1 wt% Pd-MN200 and IRA910 and initial 4-CP concentration of 100  $\mu\text{M}$ . The adsorption tests were carried out in the absence of hydrogen gas, and the reduction results are based on the loss of 4-CP due to HDC.

**Table 3**

Adsorbed amounts of 4-CP ( $\mu\text{M}$ ) at the end of the catalytic reduction for different initial 4-CP concentrations. The adsorbed 4-CP was only detected when 4-CP initial concentration was above 1.5 mM. Other reaction conditions: 25 mg of 1 wt% Pd catalyst loading at pH = 7.

Initial 4-CP concentration mmol L <sup>-1</sup>	Catalyst		
	Pd/MN200	Pd/MN100	Pd/IRA910
0.1	0.0	0.0	0.0
0.5	0.0	0.0	0.0
1.0	0.0	0.6	0.0
1.5	9.4	14.0	2.6
2.5	38.4	37.1	60.1
5.0	287.0	255.0	87.6
7.5	546.8	510.8	123.9

where  $r_0$  ( $\text{mmol g}_{\text{Pd}}^{-1} \text{h}^{-1}$ ) is the initial reaction rate,  $[4\text{-CP}]_0$  is the initial 4-CP concentration ( $\text{mmol L}^{-1}$ ) and  $k_r$  ( $\text{mmol g}_{\text{Pd}}^{-1} \text{h}^{-1}$ ) is the intrinsic rate constant (see model derivation steps in SM).

To test the kinetic model and to investigate the relative contribution of 4-CP adsorption and surface reaction to the hydrodechlorination, the influence of 4-CP initial concentration was evaluated. The initial reaction rate was measured for various initial 4-CP concentrations from 0.1 to 7.5 mM. The initial rates were calculated based on the solution phase concentrations, where the loss of 4-CP from the suspension is due to both reaction and adsorption. The desorption results at the end of each reaction showed that with increasing initial 4-CP concentration, the amount of 4-CP adsorbed on the catalysts during reaction also increased (Table 3).

In general,  $r_0$  increased with increasing initial 4-CP concentration for all the catalysts, and it followed the order of  $\text{MN200} \geq \text{MN100} > \text{IRA910}$  over the entire range of the tested concentrations (Fig. 9). The L-H model (Eq. (9)) fits well initial reduction rate versus initial concentration ( $R^2 > 0.99$ , Table 4). Comparable intrinsic rate constants  $k_r$  were obtained for the MN200 and MN100 catalysts. The values of the equilibrium adsorption constant  $K_1$  for MN200 and MN100 were almost equal, in agreement with their

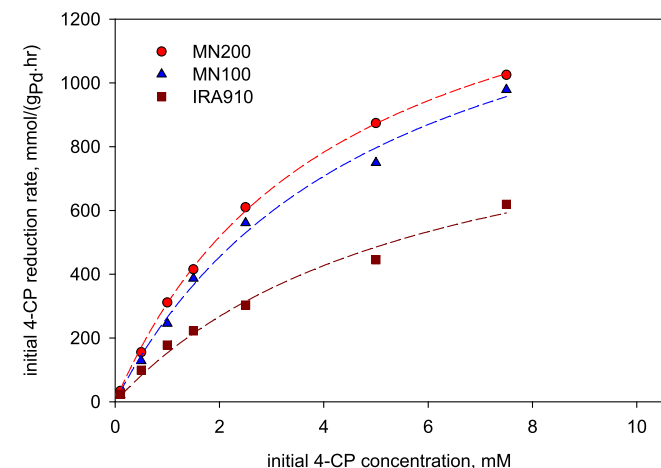


**Fig. 9.** Influence of initial 4-CP concentration on the initial rate of 4-CP reduction by 25 mg of 1 wt% Pd catalysts at pH = 7. Dashed lines are fitting curves to the kinetic model.

**Table 4**

Fitting parameters of the L-H model for 4-CP reduction at pH = 7 with 25 mg of 1 wt% Pd catalyst loading.

Catalyst	$k_r$ mmol $\text{g}_{\text{Pd}}^{-1} \text{h}^{-1}$	$K_1$ L $\text{mmol}^{-1}$	$R^2$
Pd/MN200	$1608 \pm 33$	$0.24 \pm 0.01$	0.999
Pd/MN100	$1603 \pm 135$	$0.22 \pm 0.02$	0.993
Pd/IRA910	$1060 \pm 140$	$0.17 \pm 0.03$	0.986

similar resin structure and adsorption capacity. The values of  $k_r$  and adsorption constant obtained for Pd/IRA910 were smaller. This is because IRA910 has lower adsorption affinity for the nondissociated form of 4-CP at pH = 7.

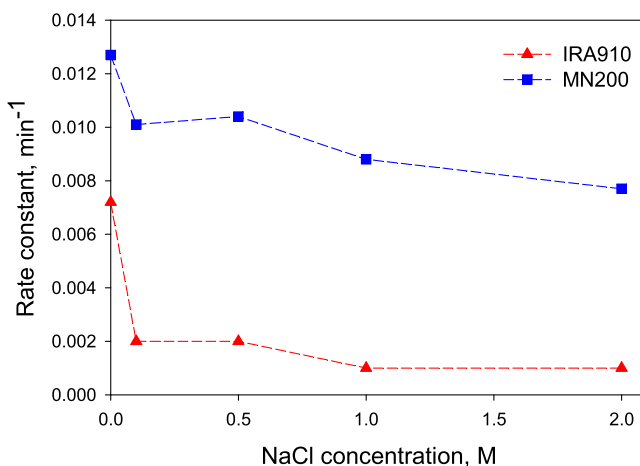


**Fig. 10.** Effect of NaCl concentration on the reactivity of the 1 wt% Pd catalysts for initial 4-CP concentration of 100  $\mu$ M, 25 mg of 1 wt% Pd catalyst loading, and pH = 7.

#### 4.7. Effect of NaCl

The reactivity of the catalysts Pd/MN200 and Pd/IRA910 was further tested in aqueous solution with varying concentrations of NaCl from 0 to 2 mol L<sup>-1</sup> at pH 7. The results indicated a more significant decrease in the rate constant of IRA910 than that of MN200 (70% vs. 20% reduction in the rate constant) when NaCl concentration was increased from 0 to 0.1 M (Fig. 10). Further increase of NaCl concentration from 0.1 to 2 M changed the catalytic activity marginally. Separate adsorption experiments in the presence of NaCl at pH 7 showed that NaCl did not have any significant influence on the adsorption of 4-CP by MN200 and IRA910. The decrease in the catalytic activity could be related to the formation of palladium chloride species (i.e.,  $\text{PdCl}_3^-$  and  $\text{PdCl}_4^{2-}$ ) and the subsequent leaching of the active sites, as reported by other studies [21,22]. The difference in the effect of NaCl on the catalytic activity of the neutral and anion exchange resins could be attributed to the anion exchange ability of IRA910, which facilitates sorption of  $\text{Cl}^-$  and hence formation of more  $\text{PdCl}_3^-$  and  $\text{PdCl}_4^{2-}$  species.

#### 4.8. Effect of Pd content

MN200 resin was loaded with three different amounts of Pd in order to investigate the effect of Pd content on the catalytic activity. The Pd nominal loadings were 0.2, 0.5, and 1 wt%, and the actual Pd contents determined by ICP-OES are 0.14, 0.44, and 0.67 wt% (Table 1). The desorption results showed that during the reduction, 4-CP adsorption was detectable on the catalysts with 0.14 and 0.44 wt% Pd (Fig. 11a), but not on 0.67 wt% Pd catalyst (Fig. 5). The amount of 4-CP adsorbed during reaction was the highest onto the 0.14 wt% Pd catalyst which increased when the reaction proceeded. The adsorbed amount of 4-CP onto 0.44 wt% Pd slightly increased at the beginning of the reaction and then decreased when reaction proceeded.

The catalyst with lower Pd contents has less available Pd sites, thus surface reaction is slower. On the other hand, adsorbed 4-CP was not observed during the reaction for the reduction of 0.1 mmol L<sup>-1</sup> 4-CP by 0.67 wt% Pd catalyst, suggesting surface reaction is faster than adsorption. Hydrodechlorination of 4-CP by 0.44 wt% Pd catalyst could be the turning point because the measured adsorbed amount of 4-CP during the reaction decreased from 15% to less than 5% of the initial 4-CP concentration as reaction progressed. The 4-CP reduction rate constants for these three catalysts are shown in Fig. 11b. The reduction rate constants were calculated based on the decay of 4-CP only due to hydrodechlorination, and

**Table 5**

Removal efficiency during the cyclic reactions, i.e., % of 1 mM 4-CP reduced by 25 mg of 1 wt% Pd catalysts after 3 h at pH 7.

Cycle	MN200	IRA910	IRA96
1	91.8	91.9	43.4
2	76.1	84.8	34.9
3	76.1	81.6	29.1
4	68.6	79.2	24.9
5	65.3	80.5	25.9
6	57.7	74.8	22.6
7	56.5	66.5	22.2
8	46.8	49.3	19.4
after regeneration	82.9	114.8	34.1

4-CP adsorption in the reaction was excluded from the total 4-CP loss. The apparent first order rate constant increased with increasing Pd content from 0.14 to 0.67 wt%. However, this increase is less significant when Pd content increased from 0.44 to 0.67 wt%, suggesting that increasing Pd content would not necessarily result in much higher reactivity. The optimum Pd content is the point where the adsorbed 4-CP during the reaction was just non-detectable, i.e., slightly above 0.44 wt%.

#### 4.9. Catalyst longevity

The reactivity of the catalysts was tested in eight sequential reaction cycles to investigate the longevity of the catalysts. 1 mmol L<sup>-1</sup> 4-CP was repeatedly spiked to the reactor at the beginning of each cycle of three hours (SM Fig. S3). Three-hour reaction was selected because less than 10% of the initial 4-CP remained in solution at the end of the first run for the most reactive catalysts (MN200 and IRA910). The repeated addition of a large amount of 4-CP to the same catalysts was selected to provide a more severe condition for testing the catalytic longevity (i.e., releasing more H<sup>+</sup> and Cl<sup>-</sup> and significant accumulation of reaction products). The catalytic activity decreased after the first run (Table 5) and gradually leveled off in the next seven runs.

The decrease in the removal efficiencies may be partly due to the loss of the catalysts during sampling (mass loss of 21% for MN200 and IRA96 and 39% for IRA910 at the end of eight cycles). When desorption of the catalysts was conducted, it was found that, although adsorbed 4-CP was not detected during the first run, significant amounts of 4-CP and phenol were adsorbed after the eight consecutive runs (Table 6). The amount of phenol adsorbed after eight runs was more than 15 times higher than that after the first run for MN200. Therefore, the accumulation of phenol in the catalysts seems to be the major reason for the loss of catalytic activity. Note that the majority of the formed phenol was still in the solution phase (Table 6). In fact, the proportion of the dissolved phenol to the total phenol was more than 95% for the anion exchange resins and ca. 70% for MN200. Separate adsorption experiments also showed that 4-CP adsorbs more strongly on the resins than phenol (SM Fig. S4), indicating the resins can be more easily regenerated after 4-CP has undergone catalytic reduction. After catalytic reduction of 4-CP, the soluble phenol can be either concentrated through multiple catalytic cycles or subjected to further treatment such as biological treatment, depending on the nature of the application.

To confirm the role of phenol accumulation on the catalyst deactivation, the catalysts were regenerated and tested again for 4-CP reduction. As shown in Table 5, MN200 regained ca. 90% of its original reactivity. Note the original removal efficiencies and the removal efficiencies after regeneration have been normalized by the catalyst weight for comparison purposes. The reactivity of the regenerated IRA910 is surprisingly higher than the original one, which could be due to resin breakage during magnetic stirring and the mitigation of external mass transfer limitation. IRA96 regained

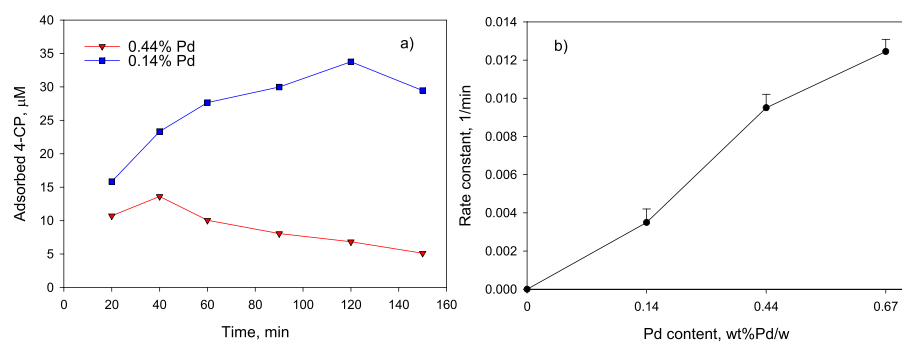


**Fig. 11.** a) Amount of 4-CP adsorbed on 0.14 and 0.44 wt% Pd/MN200 during the HDC. b) 4-CP reduction rate constants for 0.14, 0.44 and 0.67 wt% Pd/MN200. Reaction conditions: pH 7, initial 4-CP concentration of 100 μM, and 25 mg of catalyst loading.

**Table 6**

Amounts of phenol and 4-CP adsorbed (μM) by 25 mg of 1 wt% Pd catalysts after one and eight runs versus phenol concentrations (μM) in the solution phase, pH = 7.

Resin	Adsorbed 4-CP		Adsorbed Phenol		Phenol in solution phase	
	1st run	8th run	1st run	8th run	1st run	8th run
MN200	0.0	365.5	156.6	2432.9	486.1	5539.8
IRA910	0.0	47.9	0.0	266.8	622.1	6103.3
IRA96	12.1	175.7	0.0	39.2	247.6	2623.0

about 80% of its original reactivity, this could be attributed to its lower efficiency of removal of the adsorbed phenol and 4-CP from the catalysts, i.e. regeneration efficiency of 74% for IRA96 vs. 96% and 95% for IRA910 and MN200, respectively.

It should be mentioned that the catalytic activity of all catalysts did not change after three cycles if the catalysts were simply rinsed with DI water after each 3-h cycle and then mixed with fresh 1 mM 4-CP solution (SM Fig. S5). This condition is similar to real applications when catalysts are in continuous contact with fresh influent such that the accumulation of the reaction product(s) is much less. This result further verifies the ability of the catalysts to sustain their reactivity through multiple cycles by significantly eliminating the need for frequent regeneration. Moreover, the knowledge gained here will help us design new Pd/resins for reduction of organic contaminants whose reaction products have minimum adsorption affinity to the Pd/resin composite, so as to improve the stability and reactivity of the catalysts.

#### 4.10. Effect of resin structures

Overall, loading Pd on strong anion exchanger IRA910 and microporous neutral resins MN200 and MN100 was more successful than on macroporous neutral resin XAD4 and weak anion exchange resin IRA96. The Pd contents of MN200, MN100, and IRA910 were higher than IRA96 and XAD4 under the same preparation conditions (Table 1). This could be related to the higher adsorption of the Pd precursor by the microporous and strong anion exchange resins. Among the neutral resins, MN200 and MN100 showed similar reactivity. This behavior was expected as the two resins have very similar microporous structures and consequently similar adsorption behavior. The additional functional groups in MN100 did not seem to affect the catalytic reactivity. Comparing XAD4 to the other two neutral resins, XAD4 was less reactive due to a lower Pd loading. This could be associated with its lower proportion of micropores that results in lower adsorption capacity of the Pd precursor during synthesis. Among the resins, MN200 and MN100 showed the highest reactivity for hydrodechlorination of 4-CP at neutral pH where they have the highest adsorption capacity, and IRA910 had the highest reactivity at pH 11 due to its anion exchange ability (Fig. 7). Neutral resins showed stronger mechanical rigidity than IRA910 as a higher proportion of IRA910 beads

were broken apart by magnetic stirring. Our results also indicated that neutral resin MN200 was more resistant to the poisoning effect of Cl<sup>-</sup> because of the lower sorption of Cl<sup>-</sup>. On the other hand, IRA910 could be a better candidate for *in situ* regeneration because the adsorbed amounts of 4-CP and phenol onto IRA910 were much lower than those onto MN200 at neutral pH (Table 6).

## 5. Conclusions and implications

Pd-based catalysis by hydrogen gas has been considered as a promising technology for reductive destruction of various classes of contaminants. Pd-based catalysts supported on polymeric resins can be used for detoxification of adsorbed organic contaminants and for *in situ* regeneration of the spent resin. In the present work, we developed Pd-based catalysts supported on two anionic and three neutral resins, and evaluated their catalytic activity in hydrodechlorination of 4-CP. The reactivity of the catalysts was dependent on solution pH and adsorption affinity of the resins. For neutral resins, neutral pH was more favorable for reduction of 4-CP due to the inhibition effect of Cl<sup>-</sup> and H<sup>+</sup> at low pHs, however, the lack of adsorption limits catalytic reactivity at high pHs. For anionic resins, increasing pH resulted in higher reactivity due to higher sorption of 4-chlorophenolate through anion exchange. The highest reactivity of the anion exchange resins was observed at pH = 11 which is not environmentally relevant, therefore, anion exchange resins might not be suitable for typical water treatment. Nevertheless, this study provides a mechanistic insight into the catalytic reduction of a probe compound like 4-CP under a wide range of pH conditions. This would enable us to select or synthesize an appropriate resin/Pd to target contaminants of concern. For example, we used 4-CP to demonstrate that the anion exchange resins are good candidates for catalytic removal of organic contaminants that are in anionic forms under environmentally relevant pHs.

A kinetic model was developed based on the Langmuir-Hinshelwood model assuming surface reaction is the RDS. The kinetic model fit well and confirmed the enhancing effect of adsorption on the catalytic reactivity. Neutral resins are more resistant to the poisoning effect of Cl<sup>-</sup> than ionic resins because the anion exchange nature of the latter facilitates adsorption of Cl<sup>-</sup> and thus formation of more PdCl<sub>3</sub><sup>-</sup> and PdCl<sub>4</sub><sup>2-</sup> species. Adsorption of phenol over multiple reaction cycles resulted in the activity loss, and

the regeneration of the used catalysts largely restored the catalytic activity.

This study shows that the integration of adsorption and catalytic treatment is a promising strategy to significantly reduce the volume of the secondary waste from resin regeneration. Also, polymeric resins are a great candidate for developing new Pd-based catalysts due to their designable structures and unique physical and chemical properties that allow simultaneous removal of target contaminants and *in situ* regeneration of the spent resin. Future work should be carried out to examine if it is beneficial to run adsorption and catalytic reduction in sequence. In other words, Pd/resin catalysts will be used as adsorbents first and then H<sub>2</sub> will be passed through the saturated Pd/resin to initiate catalytic reduction. This might decrease the need for H<sub>2</sub> consumption and increase treatment efficiency. Future work is also warranted to grow Pd nanoparticles with better size control on resins.

## Appendix A. Supplementary data

Supplementary data associated with this article can be found, in the online version, at <http://dx.doi.org/10.1016/j.apcatb.2016.12.068>.

## References

- [1] V. Gupta, I. Ali, V. Saini, Environ. Sci. Technol. 38 (2004) 4012–4018.
- [2] Y. Lan, L. Yang, M. Zhang, W. Zhang, S. Wang, ACS Appl. Mater Interfaces 2 (2009) 127–133.
- [3] J.B. Hoke, G.A. Gramicciioni, E.N. Balko, Appl. Catal. B: Environ. 1 (1992) 285–296.
- [4] L. Calvo, M. Gilarranz, J. Casas, A. Mohedano, J. Rodríguez, J. Hazard. Mater. 161 (2009) 842–847.
- [5] M. Pera-Titus, V. García-Molina, M.A. Baños, J. Giménez, S. Esplugas, Appl. Catal. B: Environ. 47 (2004) 219–256.
- [6] M. Czaplicka, Sci. Total Environ. 322 (2004) 21–39.
- [7] M.S. Bilgili, J. Hazard. Mater. 137 (2006) 157–164.
- [8] B. Hameed, L. Chin, S. Rengaraj, Desalination 225 (2008) 185–198.
- [9] M.A. Lawrence, R.K. Kukkadapu, S.A. Boyd, Appl. Clay Sci. 13 (1998) 13–20.
- [10] T. Vincent, E. Guibal, Langmuir 19 (2003) 8475–8483.
- [11] B.P. Chaplin, M. Reinhard, W.F. Schneider, C. Schüth, J.R. Shapley, T.J. Strathmann, C.J. Werth, Environ. Sci. Technol. 46 (2012) 3655–3670.
- [12] D.P. Barbosa, P. Tchiéta, M.d.C. Rangel, F. Epron, J. Mol. Catal. A: Chem. 366 (2013) 294–302.
- [13] Y. Yoshinaga, T. Akita, I. Mikami, T. Okuhara, J. Catal. 207 (2002) 37–45.
- [14] D. Shuai, B.P. Chaplin, J.R. Shapley, N.P. Menendez, D.C. McCalman, W.F. Schneider, C.J. Werth, Environ. Sci. Technol. 44 (2010) 1773–1779.
- [15] D. Shuai, J.K. Choe, J.R. Shapley, C.J. Werth, Environ. Sci. Technol. 46 (2012) 2847–2855.
- [16] M.G. Davie, M. Reinhard, J.R. Shapley, Environ. Sci. Technol. 40 (2006) 7329–7335.
- [17] M. Aramendia, V. Borau, I. Garcia, C. Jimenez, F. Lafont, A. Marinas, J. Marinas, F. Urbano, J. Mol. Catal. A: Chem. 184 (2002) 237–245.
- [18] M.G. Davie, H. Cheng, G.D. Hopkins, C.A. Lebron, M. Reinhard, Environ. Sci. Technol. 42 (2008) 8908–8915.
- [19] G. Yuan, M.A. Keane, Appl. Catal. B: Environ. 52 (2004) 301–314.
- [20] E. Diaz, A.F. Mohedano, J.A. Casas, L. Calvo, M.A. Gilarranz, J.J. Rodriguez, Appl. Catal. B: Environ. 106 (2011) 469–475.
- [21] M.A. Keane, ChemCatChem 3 (2011) 800–821.
- [22] G. Yuan, M.A. Keane, Catal. Today 88 (2003) 27–36.
- [23] R. Kunin, Pure Appl. Chem. 46 (1976) 205–211.
- [24] D.C. Kennedy, Environ. Sci. Technol. 7 (1973) 138–141.
- [25] B. Corain, P. Centomo, S. Lora, M. Králik, J. Mol. Catal. A: Chem. 204 (2003) 755–762.
- [26] Z. Xu, Q. Zhang, H.H. Fang, Crit. Rev. Env. Sci. Technol. 33 (2003) 363–389.
- [27] S. Deosarkar, V. Pangarkar, Sep. Purif. Technol. 38 (2004) 241–254.
- [28] M. Zhang, M. Jiang, C. Liang, Chin. J. Catal. 34 (2013) 2161–2166.
- [29] I. Dodouche, D.P. Barbosa, M.d.C. Rangel, F. Epron, Appl. Catal. B: Environ. 93 (2009) 50–55.
- [30] Y.-N. Kim, M. Choi, Environ. Sci. Technol. 48 (2014) 7503–7510.
- [31] D. Gašparovičová, M. Králik, M. Hronec, Z. Vallušová, H. Vinek, B. Corain, J. Mol. Catal. A: Chem. 264 (2007) 93–102.
- [32] D. Gašparovičová, M. Králik, M. Hronec, Collect. Czech. Chem. Commun. 64 (1999) 502–514.
- [33] C. Neyertz, F. Marchesini, A. Boix, E. Miro, C. Querini, Appl. Catal. A: Gen. 372 (2010) 40–47.
- [34] D. Gašparovičová, M. Králik, M. Hronec, A. Biffis, M. Zecca, B. Corain, J. Mol. Catal. A: Chem. 244 (2006) 258–266.
- [35] J. Liu, J.K. Choe, Z. Sasnow, C.J. Werth, T.J. Strathmann, Water Res. 47 (2013) 91–101.
- [36] A. Pintar, J. Batista, J. Levec, Chem. Eng. Sci. 56 (2001) 1551–1559.
- [37] A. Pintar, J. Batista, J. Levec, Catal. Today 66 (2001) 503–510.
- [38] P. Harriott, AIChE J. 8 (1962) 93–101.
- [39] P. Weisz, C. Prater, Adv. Catal. 6 (1954) 49.
- [40] J.B. Butt, Reaction Kinetics and Reactor Design, CRC Press, 2000.
- [41] D. Shuai, D.C. McCalman, J.K. Choe, J.R. Shapley, W.F. Schneider, C.J. Werth, ACS Catal. 3 (2013) 453–463.
- [42] M. Choi, Z. Wu, E. Iglesia, J. Am. Chem. Soc. 132 (2010) 9129–9137.
- [43] S.-S. Lin, M.D. Gurol, Environ. Sci. Technol. 32 (1998) 1417–1423.
- [44] H. Wan, R.V. Chaudhari, B. Subramaniam, Top. Catal. 55 (2012) 129–139.
- [45] M.M. Dubinin, Chem. Rev. 60 (1960) 235–241.
- [46] T. Vincent, E. Guibal, Environ. Sci. Technol. 38 (2004) 4233–4240.
- [47] B. Coq, G. Ferrat, F. Figueras, J. Catal. 101 (1986) 434–445.
- [48] I.F. Cheng, Q. Fernando, N. Korte, Environ. Sci. Technol. 31 (1997) 1074–1078.
- [49] X. Zhu, S.R. Castleberry, M.A. Nanny, E.C. Butler, Environ. Sci. Technol. 39 (2005) 3784–3791.
- [50] Y. Wang, J. Liu, P. Wang, C.J. Werth, T.J. Strathmann, ACS Catal. 4 (2014) 3551–3559.
- [51] T. Xu, Y. Cai, K.E. O’Shea, Environ. Sci. Technol. 41 (2007) 5471–5477.
- [52] G.V. Lowry, M. Reinhard, Environ. Sci. Technol. 35 (2001) 696–702.